BMC Plant Biology

RESEARCH

Open Access

Seed endophytic bacteria are involved in metal adaptation of *Orobanche lutea*: community dynamics and plant growth promotion traits

Kristine Petrosyan[1,2*], Sofie Thijs[2], Tomasz Krucon[3], Renata Piwowarczyk[4], Karolina Wiśniewska[4], Wiesław Kaca[5] and Jaco Vangronsveld[2,6]

Abstract

Background Parasitic plants are affected by various abiotic stressors including water and drought stress, fluctuations or extremes of temperature, salinity, mineral deficiencies or toxic concentrations of heavy metals in soils. While the molecular mechanisms and the ecological roles of these parasitic angiosperms have been well-studied, their responses to abiotic stress remain poorly understood. This study explores the relationship between environmental metal stress and the seed endophytic bacterial community of the holoparasitic plant *Orobanche lutea* Baumg. (Orobanchaceae).

Results Our findings reveal significant shifts in microbial community composition across different environmental conditions, developmental stages and time points. *Orobanche lutea* seeds selectively accumulate metals such as Zn and Pb. Significant differences in the *O. lutea* seed microbial community composition suggest a strong influence of both, environmental conditions and plant developmental stages. Certain bacterial genera, including *Bacillus*, *Paenibacillus*, *Pantoea*, *Okibacterium*, *Staphylococcus* and *Micromonospora* were consistently detected across all samples, suggesting a vertically transmitted core microbiome. Notably, seed endophytic bacterial communities in *O. lutea,* respond dynamically to metal stress. Several isolated strains (e.g. *Bacillus*, *Paenibacillus, Curtobacterium* and *Mictobacterium*) showed high tolerance to Zn and Pb salts. However, elevated Zn and Pb concentrations in seeds do not promote the enrichment of metal-tolerant endophytes. Furthermore, metal stress appeared to increase the frequency of plant growth-promoting (PGP) traits within the seed microbiome supporting the idea that endophytes contribute to the adaptation of holoparasitic plants to heavy metal stress.

Conclusions These results highlight the dynamic nature of seed-associated microbial communities under metal stress and underscore the critical role of seed endophytes in mediating the responses of holoparasitic plants to environmental challenges. The relationship between seed microbiome composition and metal exposure offers new insights of understanding stress resilience and developing microbial-based mitigation strategies.

*Correspondence:
Kristine Petrosyan
petrosyan@umk.pl

Full list of author information is available at the end of the article

Keywords Holoparasites, Orobanchaceae, Metal stress, Plant growth promoting bacteria, Immature and ripe seeds, Seed microbiome, Metal tolerance

Background

The rapid developments of heavy industry and resulting environmental pollution have led to large-scale transformations of landscapes. Such industrial lands often harbor a limited number of adapted plant species including some holoparasitic members of the Orobanchaceae family [1]. Parasitic plants represent a fascinating line of evolution and are often found in extreme environments –such as saline, arid, cold or polluted habitats [2]. Although numerous studies have explored the molecular mechanisms of plant parasitism and the ecological impacts of these highly specialized angiosperms, significant knowledge gaps remain regarding their responses to abiotic stress factors. However, like their hosts, parasitic plants are affected by abiotic stress factors, such as water and drought stress, fluctuations or extremes of temperature, saline soils, mineral deficiencies or toxic concentrations of heavy metals in soils [3]. These challenging conditions can alter their host preference, and stress responses may be host-dependent or -independent. Such effects may result from either direct influence through restrictions in seed germination or from host mediated factors such as limited host availability, host susceptibility to parasitism or changes in host signaling. In response to abiotic stress, parasitic plants may transfer stress-responsive metabolites and stress-induced signals to their hosts when exposed to abiotic stresses. The host plant, in turn, activates defense mechanisms, often transferring harmful compounds back to the parasites [3].

Despite obligatory interaction with their plants, parasitic plants are self-regulating organisms with own metabolic profiles that differ from their hosts [4–7]. The ability of holoparasitic plants, particularly *Orobanche* s.l., to decrease the levels of potentially toxic metals in their host plants is well documented [4]. They can thrive in metal-rich environments or in industrial waste areas, often forming large populations. Species such as *O. lutea*, *O. laxissima, Phelipanche nowackiana* and *P. nana* tend to accumulate various minerals and potentially toxic metals—such as Zn, Ni and Cd while decreasing the concentrations in the host plants [1, 8–10]. Turnau et al. (2018) [1] demonstrated that potentially toxic metals (Zn, Cd and Pb) were shared between the host plant *Medicago falcata* L. (Fabaceae) and the parasite *O. lutea,* when growing on an industrial waste land in Poland (Silesia-Cracow Upland). The concentrations of potentially toxic metals in the host plants infected by *O. lutea* were significantly lower compared to non-infected individuals of the same species. They also reported that both, parasites and metal stress, may activate several physiological and metabolic pathways in the infected host. In the case of *M. falcata* infected by *O. lutea*, increased photosynthetic capacity, enhanced mycorrhizal colonization and greater arbuscular richness were observed [1]. Similarly, a study on *Odontarrhena lesbiaca* (Brassicaceae) demonstrated that infected plants had lower Ni concentrations in their leaves than their non-infected counterparts [9].

Within the parasite-host complex, stress-responsive molecules and potentially harmful compounds, including heavy metals, are exchanged via the haustoria [11–13]. The haustorium functions like a pump, facilitating the uptake of water and solutes from the host plant to the parasite. It also absorbs osmotic compounds, such as polyol mannitol, which facilitates this flow [4].

Parasitic plants are connected to their hosts via haustoria not only for the uptake of nutrients, energy and water, but also for the exchange of endophytic microorganisms [14]. In general, bacterial secretions such as indole-3-acetic acid (IAA), organic acids, siderophores, and ACC-deaminase contribute to enhance the availability of nutrients for plants [15]. In this context, endophytic bacteria play an important role in understanding the uptake mechanisms of heavy metal ions and in supporting plant tolerance to metal toxicity. They can decrease metal accumulation in plant tissues and reduce bioavailability of metals in the soil through various mechanisms [16]. Additionally, exposure to metals has been shown to promote the migration of specific endophytes to the aboveground parts of the plant [17].

In this study, we investigated the endophytic bacterial microbiome richness and diversity of *O. lutea* seeds in various developmental stages and their plant growth promoting (PGP) traits under metal stress. The results provide essential evidence highlighting the importance of the seed endophytic bacterial diversity of this species. Specifically, we investigated modifications in bacterial communities during seed maturation across two consecutive generations and examined how bacterial diversity and the potential PGP traits of the endophytic bacteria were affected by metal stress. We hypothesized that toxic metal concentrations in the soil may influence both the composition of the seed endophytic community of *O. lutea* and the dynamics of this community during seed maturation. Furthermore, these bacteria possess PGP traits that contribute to an abatement of the metal stress experienced by their host.

To verify our hypothesis, we employed arrange of interdisciplinary methods, including microbiological, molecular, biochemical, spectroscopic, bioinformatic and statistical approaches.

Material and methods

Study design

Sampling was conducted over two consecutive growing seasons at two distinct locations in Poland: a metal-polluted site and a non-polluted reference site. The heavy metal polluted site (HM) is characterized by elevated concentrations of zinc (Zn), nickel (Ni) and lead (Pb) [18] while the other, non-polluted (NHM), served as a reference site. At each site, seeds of *O. lutea* were collected at two developmental stages: immature and ripe. To assess the impact of environmental pollution on seed-associated microbial communities, the study included both culture-dependent and molecular methods.

Element concentrations in seeds were quantified using ICP-OES in order to assess metal accumulation patterns in seeds. Microbiome profiling was performed using high-throughput sequencing to characterize bacterial communities associated with seeds. To evaluate the functional relevance of isolated strains in polluted environments, metal tolerance assays were conducted. In parallel, culturable bacterial isolates were obtained and screened for plant growth-promoting (PGP) traits such as ACC deaminase (ACCD) activity and production of indole-3-acetic acid (IAA), organic acids (OA) and siderophores (SID).

This multifactorial design allowed us to compare microbial composition, functional traits, and metal uptake between polluted and non-polluted origins, across different seed maturity stages and throughout two consecutive generations.

Site description and sampling of Orobanche lutea

The polluted site (HM) is located in the Silesia-Cracow Upland, Ząbkowice, Dąbrowa Górnicza district. It is situated at the edge of a forest, along a path bordering meadow wastelands created after the exploitation of calamine- an ore rich in heavy metals. The site coordinates are 50°22′07″ N, 19°16,53″ E., at an elevation of 325 m a.s.l. (Fig. 1A).

The region hosts some of the largest Zn, Ni and Pb deposits in Europe [18]. The soil in this region is typically calcareous (pH 7.3) and supports a variety of metal tolerant plant species, providing favorable conditions for the growth of *O. lutea* [1, 18]. Previous detailed analyses did not show significant differences in pH value (ranged between 6.4 and 7.3) of the soil at both locations (polluted and non-polluted) [1]. The historical exploitation of calamine rich in Zn, Pb and silver (Ag) may have contributed to the prolific development of *O. lutea* populations [1]. A detailed analysis of toxic metal and nutrient concentrations in the polluted soil from Silesia-Cracow Upland and the non-polluted soil from the Ponidzie regions can be found in Turnau et al. (2018) [1], who showed substantial differences in metal concentrations between the polluted and non-polluted sites, especially for Cd and Zn. High levels of heavy metal concentrations in soil and in plants from this site have been confirmed by Turnau et al. (2018) [1] and Wiśniewska et al. (2025) [19]. Moreover, this site and the surrounding area is characterized by a high level of industrialization and air pollution, and is already known for centuries as one of the largest zinc and lead deposits in Europe [20–23].

The non-polluted site (NMH), Ostra Góra is located within the Ponidzie region, in the mesoregion of the Pińczowski Garb (Świętokrzyskie Voivodeship), far from industrial areas. In the Świętokrzyskie Voivodeship, no exceedances of the permissible values for Cd, Zn and other heavy metals have been recorded. Additionally, among the analyzed trace elements, no trend of their accumulation in soils has been observed at least over the past 15 years [24]. The site is situated at 50°26′36.0″ N 20°47′05.0" E, at an elevation of 265 m a.s.l. and this is characterized by typical xerothermic grassland vegetations (Fig. 1B) [18].

Historical monthly climate data for the study sites were obtained from WorldClim 2.1, downscaled from CRU-TS 4.06 [19]. For each site, annual minimum and maximum temperatures and total annual precipitation were recorded. The polluted site was characterized by slightly higher minimum temperatures and precipitation, whereas the unpolluted site exhibited higher maximum temperatures [19].

Plant material and identification

All experimental procedures in this study including the field studies, collection of plant material, were conducted in strict accordance with local, institutional, national and international guidelines and legislation, and necessary permits were obtained. The collection of *O. lutea* seeds was conducted with permission no. WPN.I.6400.3.1.2021.AD (Ostra Góra) and WPN.6400.4.2021.MS1.1 (Dąbrowa Górnicza) issued by the Regional Directors for Environmental Protection in Poland accordance with Polish and EU biodiversity legislation. The field collection of seeds was performed by Renata Piwowarczyk and Karolina Wiśniewska (Institute of Biology, Jan Kochanowski University, Kielce, Poland). Renata Piwowarczyk also conducted the formal taxonomic identification of the species. The plant names were updated based on the International Plant Names Index (IPNI) [25].

The voucher specimen has been deposited in the Herbarium of Jan Kochanowski University in Kielce (KTC), Poland (acronym according to Thiers) [26]. The collection is not numbered, but the herbarium sheets are stored in a separate section under the name "Parasitic plants", and the species are sorted alphabetically, in boxes labeled with the species name.

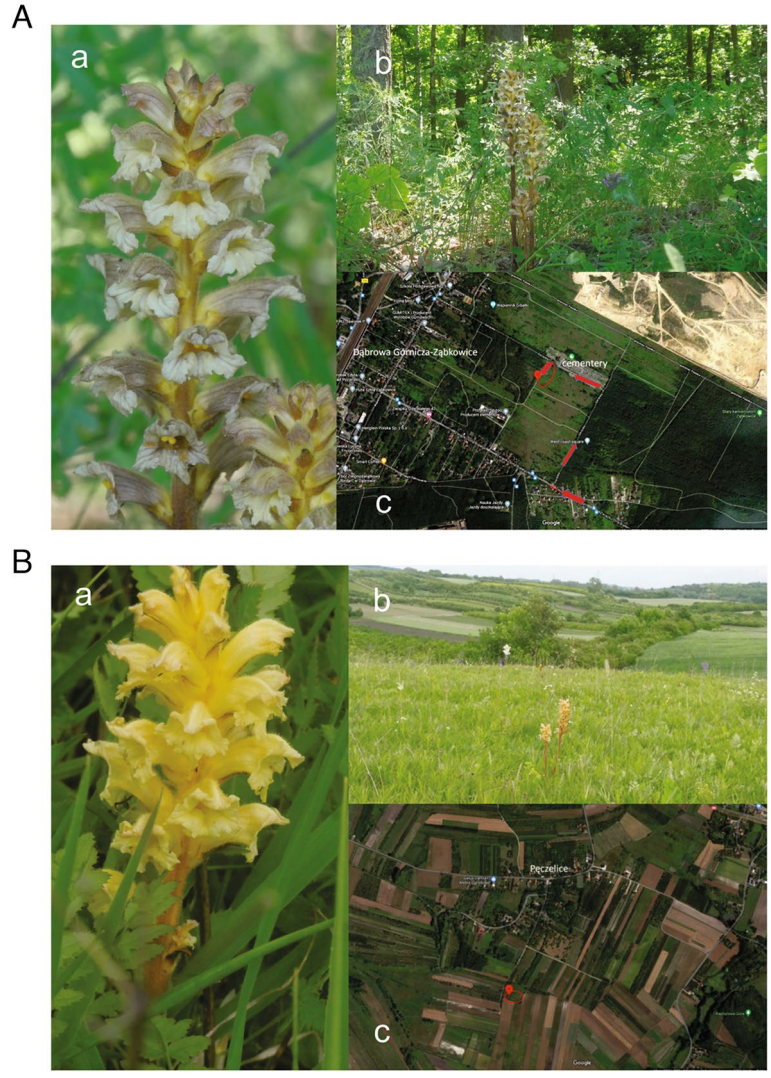

Fig. 1 **A** (**a**) General habit of *Orobanche lutea* from the polluted site; (**b**) The polluted habitat in Ząbkowice, Dąbrowa Górnicza district, and 200 m from the cemetery at Górzysta Street, the edge of the forest by the path and the meadows and wastelands. Photos by K. Petrosyan. (**c**) Satellite image of the study site obtained from the Google Earth; image modified by R. Piwowarczyk. 1 **B:** (**a**) General habit of *Orobanche lutea* at the non-polluted site, (**b**) The non-polluted site in Ostra Góra, south of Pęczelice (Busko-Zdrój), xerothermic grasslands. Photos by K. Petrosyan. (**c**) Satellite image of the study site obtained from the Google Earth: image modified by R. Piwowarczyk

Sampling of seeds

Orobanche lutea is one of the most abundant representatives of the genus *Orobanche* in Poland [18]. Despite the high density of populations in some regions of Poland – such as the Silesia-Cracow Upland—*O. lutea* is classified as a species under partial legal protection in Poland and has been included in several regional red lists [22, 27, 28]. *Orobanche lutea* is an oligophagous species (infecting host species belonging to one taxonomic family) parasitizing on the genus *Medicago* (family Fabaceae). It commonly infects the species *M. falcata*, *M. sativa* and the hybrid *M.* × *varia* which are the typical hosts of *O. lutea* populations across Europe [18, 22, 29]. The young (immature) seeds of *O. lutea* were collected from both sampling sites in May–June in the years 2021 and 2022. Portions of the closed ovaries were stored in aseptic conditions for subsequent experiments, while additional samples were preserved in 99% glycerol at −80°C. Mature seeds were collected from opened capsules of fully developed plants in June-July of the same years. The collected mature seeds were air-dried.

Morphological observations of both young and ripe seeds of *O. lutea* were conducted using a Nikon SMZ-800 stereoscopic microscope coupled with a Nikon DSFi3 camera (Tokio, Japan) (Fig. 2).

Elements analysis in the seeds by ICP-OES

The concentrations of the elements in seeds were determined by Inductively Coupled Plasma Optical Emission Spectrometry (ICP-OES, Agilent Technologies 700

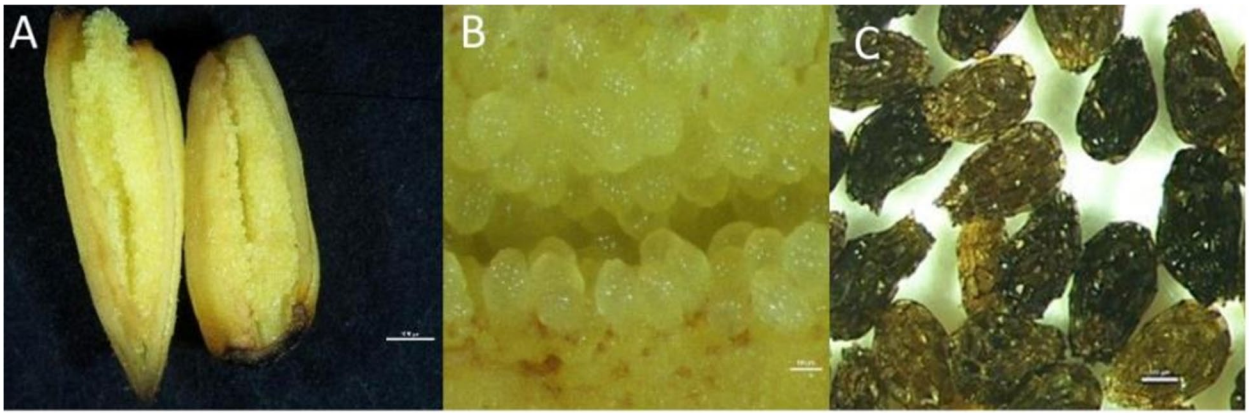

Fig. 2 Nikon SMZ-800 stereoscopic microscope images of *Orobanche lutea* seeds: **A** young seeds within the ovary (longitudinal section) (1:1000), **B** young seeds (1:100), **C** ripe seeds (1:500). Photos by K. Zubek

Series, Australia) using standard method described by Thijs et al. (2018) [30]. Fifty mg of dried ripe seeds of *O. lutea* were rinsed with distilled water and dried in an oven (105 °C) and chipped. After the dried seeds were hammer-milled (Retsch SM100) to obtain a fine powder. Samples were wet digested in Pyrex tubes in a heating block overnight in Suprapur 14 N HNO_3 (1 mL) at 40 °C, followed by a hot digestion at 110 °C. After 3 times drying, the samples were cooled down and resolved in 1 mL HCl Suprapur 37%. The samples were dried again in the heating block at 110 °C. When dry, the samples were dissolved in 10 mL 2% HCl [30]. Blanks of reagents (concentrated acids) and standardized reference samples (Trace Elements in Spinach Leaves 1570a, NIST, U.S.) were included. All analyses, including blanks and reference material were performed in three replicates ($n = 3$). The experimental data were statistically analyzed using the Microsoft Office Excel program. The concentrations of minerals and metals were expressed as $\mu g \times L^{-1}$. The results were expressed as a mean of the triplicates with ± standard error (SE) and standard deviation (SD). The element concentrations are expressed on dry weight (dw) of plant tissue.

Seed surface sterilization and homogenization

The aim of the seed surface sterilization procedure was to obtain only the endophytic communities of the seeds. This was performed according to the protocol by Petrosyan et al. (2022) [31]. For each sampling location and year, 50 mg of young and ripe seeds of *O. lutea* were collected per replicate, using a design of 8 samples in 4 replicates.

Sterilization efficiency was confirmed using both microbiological and molecular approaches. 100 µL of the last rinsing water was planted on Petri dishes containing 869 rich medium (0.035gL^{-1} $CaCl_2 \cdot 2H_2O$, 0.5gL^{-1} NaCl, 1.0gL^{-1} $MgSO_4 \cdot 7H_2O$, 1gL^{-1} Tryptone, 0.5gL^{-1} Yeast extract, 0.1gL^{-1} D (+)-glucose, 15gL-1 Agar, pH 7.0) and incubated for 5 days [32]. DNA was also isolated from the rinsing water using the AX Bacteria Spin kits (A&A Biotechnology, Gdynia, Poland) and analyzed via standard PCR with universal 16S rDNA primers (Com1/Com2). Deionized water served as a negative control. Absence of bacterial colonies on the plates and PCR products confirmed successful sterilization.

The surface sterilized seeds were homogenized in 0.5mL 10mM $MgSO_4$ using a sterile pellet pestle (Kimble®). To complete the homogenization and obtain a homogeneous suspension, 5–6 metal stainless steel ball beads were added (2.8 mm) and the mixture was shaken using a two-bladed mixer mill (Retsch MM400, Germany) for min at 25 Hz. The homogenate was then divided: one portion was used for DNA extraction, and the other for growing culturable bacteria.

Molecular analysis of the endophytic bacteria

Isolation of bacterial DNA and 16S rRNA amplicon sequencing

To assess both cultivable and uncultivable bacterial diversity of the seeds, fractions of the homogenized suspensions of the surface sterilized seeds were used. DNA was extracted from the seed homogenate in 4 replicates using the Mobio PowerPlant protocol based on the PowerPlant® Pro DNA Isolation Kit and patented solution (Inhibitor Removal Technology® IRT). For isolation of high-quality DNA from seeds, 450 µL of Bead Solution (181mM $NaPO_4$, 121mM guanidinium thiocyanate, pH 7) was added to the seed homogenate, followed by 50µL of C1 solution (150 mM NaCl, 4% SDS, 0.5 M Tris, pH 7), 30 µL lysozyme (10 mg mL^{-1} H_2O) and incubation at 37 °C for 15 min. Afterward, 5 µL proteinase K (100 mg mL^{-1}) was added, followed by incubation at 58 °C for 20 min. Then, 3 µL RNAse A solution (25 mg mL^{-1}) was added and briefly vortexed. Subsequently, a 500 µL equal volumes of phenol: chloroform: isoamyl alcohol (pH 6–8) was added and vortexed until no biphasic layer remained.

The samples were lysed at 25 Hz for 5 min using a shredder (Retsch MM400), centrifuged for 2 min, and 450–500 µL of supernatant were transferred to clean 2mL tubes and resuspended in 175 µL of patented solution PD3 (Inhibitor Removal Technology® IRT) for removal of PCR inhibitors from plant extracts. The tubes were vortexed for 5 s and then incubated at 4 °C for 5 min avoiding the pellet move. 600 µL supernatant was transferred into clean 2 mL tubes. Finally, 600 µL of C4 (5 M guanidine hydrochloride, 30 mM Tris, 9% isopropanol, pH 6.8), 600 µL of 100% absolute ETOH were added and vortexed for 5 s 750 µL were loaded onto the spin filter, centrifuged at 10,000 rpm for 30 s 500 µL of C5 (10 mM Tris, 100 mM NaCl, 50% ETOH pH 7.5) were added to spin filter, centrifuged for 30 s at 10,000 rpm. The DNA pellet was washed with 500 µL of 100% ETOH and centrifuged for 30 s at 10,000 rpm. To remove residual ETOH, the samples were centrifuged for 3 min at maximum speed. Finally, isolated DNA samples were carefully placed into a new clean 1.5 mL Eppendorf and twice 40µL of elution buffer C6 (10 mM Tris, pH 8) added. DNA samples were quality checked using a Nanodrop 2000 (Thermo Fisher Scientific, Wilmington, DE, United States). Part of the DNA was stored at −20 °C, and the rest was used for 16S rRNA amplicon sequencing. Library preparation and Illumina sequencing were done as described by Petrosyan et al. [33].

Bioinformatic processing of reads

Raw reads were demultiplexed using Illumina MiSeq software and processed using the DADA2 package 1.10.1 [34] in R version 4.1.4. Parameters for length trimming were set to keep the first 290 bp of the forward read and 200 bp of the reverse read, maxN = 0, MaxEE = (2,5), and PhiX removal. Error rates were inferred, and the filtered reads were dereplicated and denoised using the DADA2 default parameters. After merging paired reads and removal of chimeras via the RemoveBimeraDenovo function, an amplicon sequence variant (ASV) table was constructed. Taxonomic assignment was done using the SILVA v138 database [35, 36]. The resulting ASVs and taxonomy tables were combined with the metadata file into a phyloseq object (Phyloseq, version 1.26.1) [37]. Contaminants were removed using Decontam (version 1.2.1) applying the prevalence method with a 0.5 threshold value [38]. The ASV table was further processed removing organelles (chloroplasts, mitochondria) and prevalence filtered using a 2% inclusion threshold (unsupervised filtering) as described by Callahan et al. (2016) [34].

Data visualization and statistical analyses

Alpha-diversity indexes (Simpson, Shannon) were calculated on unfiltered data using MicrobiomeSeqscripts. ANOVA and Tukey Honest Significant Differences (Tukey HSD) was applied for hypothesis testing; where assumptions of normality and homoscedasticity were not met, Kruskal–Wallis Rank and Wilcoxon tests were used. The results were summarized in boxplots and relative abundances were calculated and visualized in bar charts using Phyloseq. All performed statistical tests were corrected for multiple testing and alpha < 0.05 was considered statistically significant. All graphs were generated in R version 4.1.4.

Beta-diversity assessed using the Bray–Curtis dissimilarity matrix after transforming the data into relative abundance and visualized using Principal Coordinate Analysis (PCoA) and Canonical Analysis of Principal Coordinates (CAP). Differences between samples were evaluated using the anosim, adonis, and betadisper functions from the Vegan package (version 2.5–7).

Genomic DNA extraction and taxonomic identification of the culturable endophytic bacterial strains

The first aliquot of the homogeneous suspension of surface sterilized seeds was used for DNA extraction, the second for isolation of culturable bacteria. In order to cultivate diverse endophytic bacteria, 100 µL of the seed suspension were put onto 1/10 diluted 869 (rich) media and incubated at 30 °C for 7 days. For further experiments, single, morphological diverse colonies were picked and purified. The pure colonies were used for further experiments. DNA isolation was performed using a standard procedure for DNA isolation from bacterial pellets using an ABI MAGMAX automated DNA extraction system. DNA was quantified with a Qubit® 2.0 Fluorometer (Thermo Scientific, US) and verified for purity on a Nanodrop 2000 (Thermo Fisher Scientific, Wilmington, DE, United States) spectrophotometer with an A260/A280 ratio of 1.7–2.0. The near full-length sequences of the 16S rRNA gene were amplified with the primers 27f (5'-AGAGTTTGATCCTGGCTCAG-3') and 1492r (5'-GGTTACCTTGTTACGACTT-3') [39]. The products were verified on agarose gel and shipped to Macrogen for 16S rRNA Sanger sequencing. Sequences were processed in Geneious v4.8 and were analyzed over the ribosomal database SILVA (https://www.arb-silva.de/aligner/).

Ribosomal RNA gene sequences were compared with reference sequences from the GenBank databases, using the Ribosomal Database Project (RDP) website (http://rdp.cme.msu.edu/), Basic Local Alignment Search Tool (BLAST) software (http://blast.ncbi.nlm.nih.gov/Blast.cgi). The isolates were assigned to species or the highest best taxonomic rank possible.

Metal tolerance test

The isolated bacterial strains were evaluated for their metal tolerance ability using liquid 869 rich medium enriched by varying concentrations of lead ($PbCl_2$)

and zinc ($ZnSO_4 \cdot H_2O$) salts with 1.0 mM $PbCl_2$ and $ZnSO_4 \cdot H_2O$ 0.6 mM, 1.0 mM, 2.0 mM and 2.5 mM [40]. The assay was performed in three replicates. After 5 days of incubation, bacterial growth was evaluated as a (-) no growth and (+) growth.

In vitro plant growth promoting (PGP) traits of isolated endophytes

The bacterial strains isolated from the ripe seeds of *O. lutea* were screened for their plant growth-promoting (PGP) traits in vitro. All assays were performed at least two times. The assays were performed using two technical replicates for each isolate. The outcomes of the PGP trait assays were evaluated qualitatively and recorded as binary results (positive/negative) based on the presence or absence of the respective phenotypic response.

IAA production was assessed using the Salkowski after cultivation in 1/10 869 medium [32] supplemented with 20mL L-tryptophan per 0.5L [41]. Organic acid production was tested following Cunningham and Kuiack (1992) [42]. ACC-deaminase activity was evaluated in SMN medium with 5 mM ACC as N-source [43]. Production of siderophores was evaluated using 284 media with 0.25 µL iron and CAS solution and with 0 µl of Fe as control [44]. Detailed methods were presented in Petrosyan et al. (2022) [31].

Results

Elements concentrations in seeds

In the seeds collected from the polluted site (HMSd) prominent enrichments of Fe and Mn (Fig. 3A) were observed. Concentrations of Zn, Cu and Pb were obviously higher in seeds from the polluted site (HMSd). Mo concentrations were below the detection limit. Pb concentrations were high in seeds from polluted site (HMSd). However, in seeds from the polluted site (HM) lower concentrations of Ni and Cr were found compared to non-polluted site (NHM) (Fig. 3B).

Total bacterial communities of young and ripe seeds of Orobanche lutea growing on metal polluted and non-polluted sites

In total 36,839 high-quality sequences were obtained from Illumina MiSeq sequencing, resulting in 244

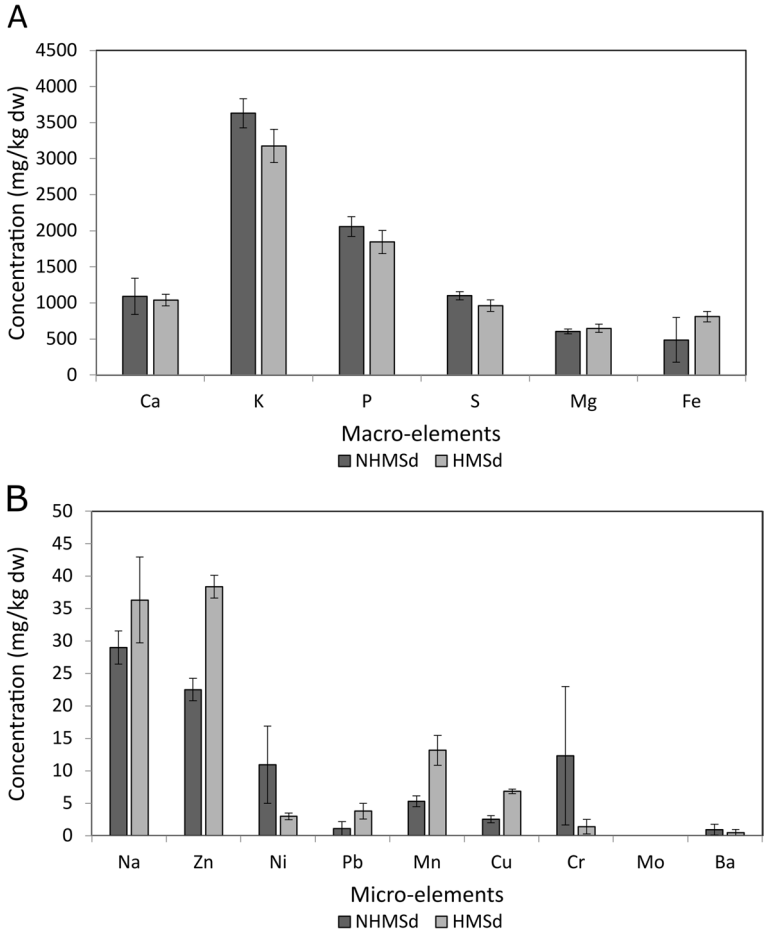

Fig. 3 Element concentrations in seeds of *Orobanche lutea*. **A** macro-elements concentrations in seeds (NHMSd vs HMSd). **B** micro-elements concentrations in seeds (NHMSd vs HMSd). Presented are mean values ± SD or SE ($n = 3$)

amplicon sequence variants (ASVs) across all libraries from *O. lutea* seeds collected at the polluted ($n = 8$ plants) and reference ($n = 8$ plants) sites. Among the 11 identified bacterial phyla, the relative abundance profiles of dominant bacterial phyla (> 1%) revealed that all seed samples were consistently dominated by Pseudomonadota, Bacillota, and Actinomycetota, although their proportional contributions varied significantly among developmental stages and years (Fig. 4). Low abundance phyla, including Planctomycetota and Fusobacteriota, were detected and contributed marginally to the overall community composition (> 1%), therefore, they were considered major divers of community differences among seed samples.

Alpha diversity metrics demonstrated pronounced differences among seed groups (Fig. 4). The lowest alpha diversity (Observed richness, Shannon and Simpson indices) was recorded in young seeds from the polluted site in both years (PY 2021, PY 2022) and young seeds from non-polluted site in 2022 (NPY2022) in contrast to Non-Polluted-Young-2021 (NPY2021) (Fig. 4A).

Shannon–Wiener diversity analyses shown significant differences between young and ripe seeds from polluted sites in 2021 (PY2021 vs. PR2021), indicating seed developmental stage and environmental effects (Fig. 4B). In contrast, alpha diversity patterns in 2022 were more uniform across treatments. These findings suggest that year-to-year variation and seed maturity are key factors influencing microbial composition.

Taxonomic composition varied between years and seed maturity stages. Seeds collected in 2021 exhibited a higher abundance of Bacillota across most samples. This indicates that Bacillota played a dominant role in the microbial communities during that year, in seeds from both polluted and non-polluted sites. However, in 2022,

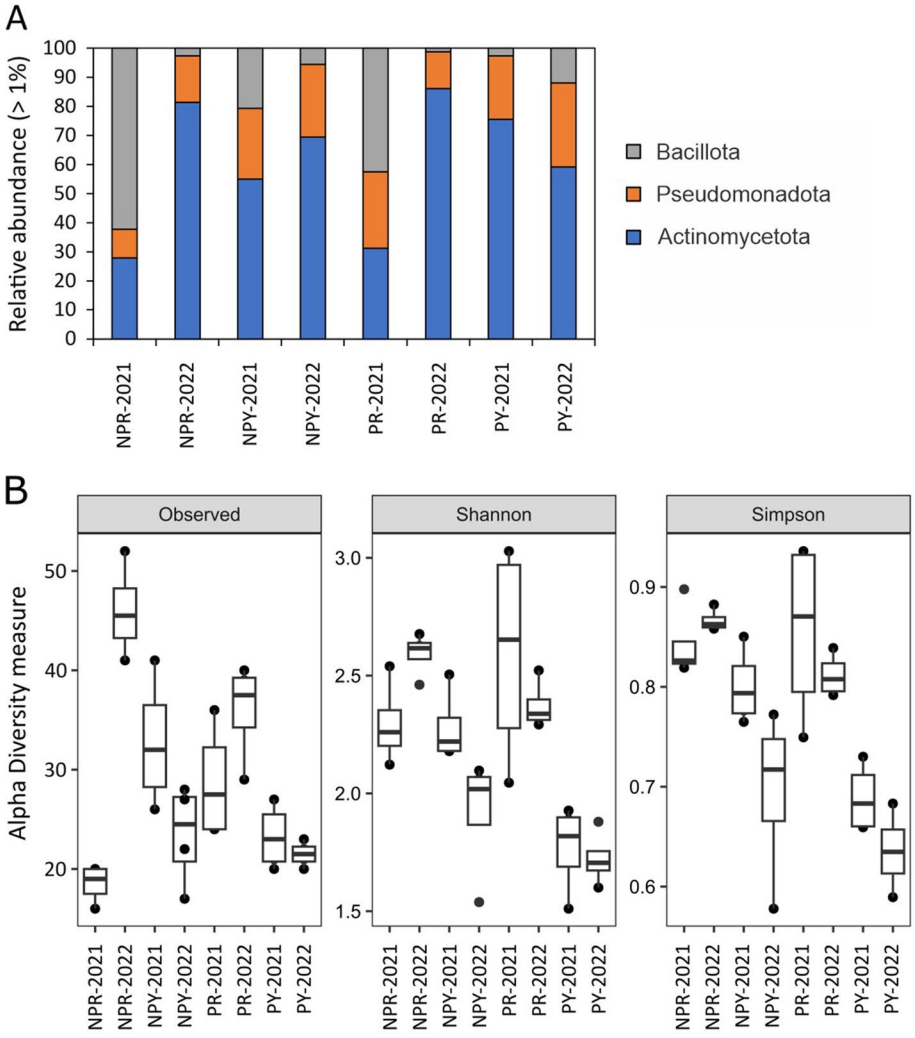

Fig. 4 **A** Relative abundance of bacterial phyla (> 1%) in young (Y) and ripe (R) seeds of *Orobanche lutea* from polluted (P) and non-polluted (NP) sites across two experimental years (2021 and 2022). **B** Pairwise comparisons of Illumina MiSeq™ sequencing reads analyzed using the Wilcoxon rank sum test, showing p. adjust values greater than 0.05 for diversity indices (Observed ASVs, Shannon and Simpson)

Pseudomonadota were the dominant phylum, particularly γ-Proteobacteria in Polluted-Ripe 2022 (PR2022); Bacillota were lower. These shifts highlight a temporal restructuring of microbial communities from 2021 to 2022, with Bacillota declining and Pseudomonadota increasing in relative abundance (Fig. 4A).

Ripe seeds, irrespective of the site, were largely dominated by α-Proteobacteria in both years. Ripe seeds from the polluted site in 2022 (PR2022) exhibited a strong presence of γ-Proteobacteria, and a markedly decline in Bacilli. In young seeds from polluted sites (YP), γ-Proteobacteria, Bacilli, and Actinomycetes were prominent, while in young seeds from the non-polluted site (NPY), γ-Proteobacteria and Bacilli were the most abundant. Interestingly, in young seeds from polluted sites in 2022 (PY2022) Actinomycetes were dominating, while Bacilli were less abundant.

Based on unconstrained ordination using the Bray–Curtis dissimilarity we observed that samples NPR2021 and PR2021 are more diverse compared to the sample groups PR2021 – NPR2021, NPR2022 – PR2022, and NPY2022 – PY2022. Grouping by site, ripeness and year of collection was statistically significant (ANOSIM p- value < 0.05) but not strong (ANOSIM R = 0.3718) explaining about 38% of the differences in distances (ADONIS R2 = 0.388). Significant differences were detected between young and ripe seeds groups from the non-polluted site only (q-value < 0.05). Also dispersion analysis further indicated that seed maturity significantly influenced community variability (BETADISPER p-value < 0.05) (Fig. 5).

Canonical Analysis of Principal Coordinates (CAP) showed temporal and environmental effects on the seed microbiota. Bacillota, particularly *Paenibacillus*, were prominent in ripe seeds from the polluted site. The genus *Stenotrophomonas* was more abundant in ripe seeds from the non-polluted (NPR) site in comparison to ripe seeds from the polluted site (PR) and young seeds from the non-polluted site (NPY) (Fig. 5).

Diversity and in vitro PGP activities of isolates

Using homogenized suspensions of surface-sterilized seeds and 16S rRNA Sanger sequencing, the cultivable endophytes of young and ripe seeds of *O. lutea* populations from metal polluted and non-polluted sites were isolated, identified and tested for their PGP traits. Our analyses indicated a diverse microbial occurrence across different seed types and conditions. A total of 231 bacterial strains belonging to the main bacterial phyla Bacillota, Pseudomonadota and Actinomycetota were isolated and identified using the NCBI taxonomy browser. 65% of all cultivable seed isolates belong to the Bacillota with the class Bacilli. The remaining isolates belong to α- and γ-Proteobacteria (10.35%), Actinomycetia (11.65%) and unclassified bacteria (13.0%) (Table 1). The bacterial group "Other/Unclassified" represents bacterial taxa that could not be assigned at lower taxonomic levels due to limited reference information.

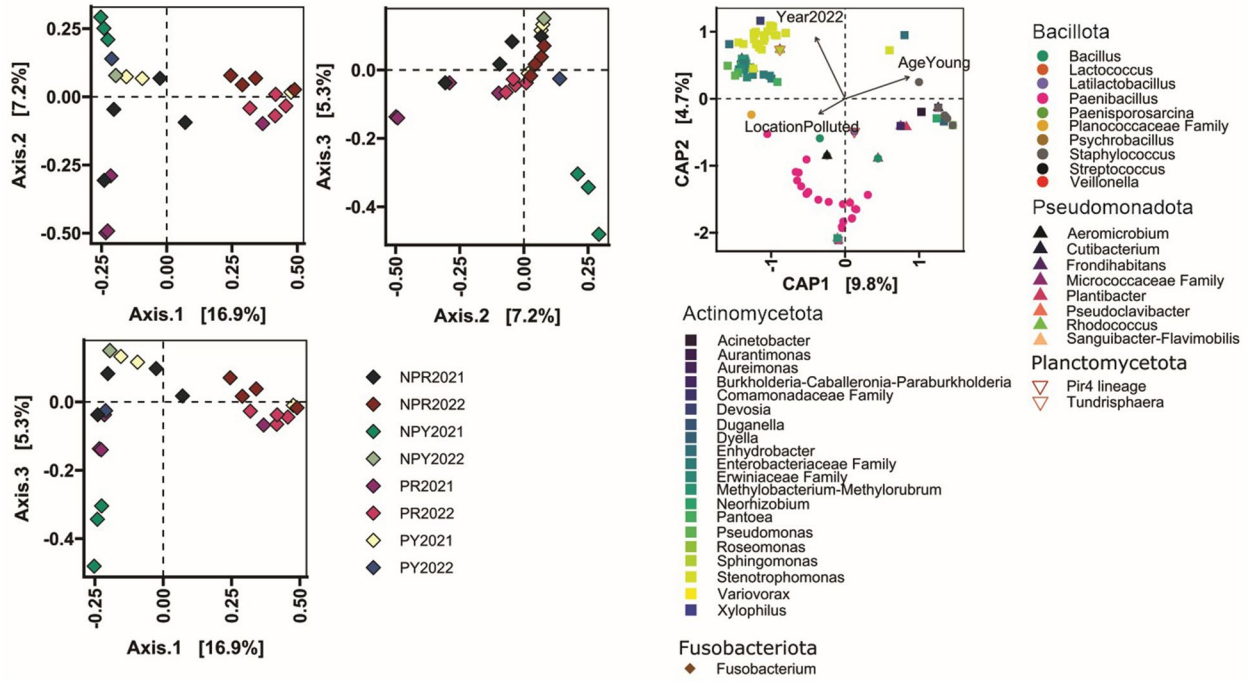

Fig. 5 Canonical Analysis of Principal Coordinates (CAP) highlighting the variations in microbial community structure of *Orobanche lutea* seeds

Table 1 Cumulative list of the cultivable endophytic bacteria in the young and ripe seeds of *Orobanche lutea* in non-polluted and metal polluted soils and their taxonomic information

Phyla	Class	Order	Genus	Count of isolated bacteria %
Bacillota	Bacilli	Bacillales	*Bacillus*[1**, 2**]	65%
			Priestia[2*,2**]	
			Peribacillus[2*,2**]	
			Staphylococcus[1*,2*]	
			RisungbinellaUncultured[1*, 1**]	
			Exiguobacterium[1*, 1**]	
`		Paenibacillales	*Paenibacillus*	
Actinomycetota	Actinomycetia	Micrococcales	*Micromonospora*[1**,2**]	11.65%
			Okibacterium[1*,2**]	
		Actinomycetales	*Curtobacterium*[1*, 2*]	
		Micrococcales	*Brevibacterium*[2*,2**]	
			Promicromonospora[2*,2**]	
		Actinomycetales	*Kocuria*[2**]	
		Micrococcales	*Plantibacter*[1*,2*]	
			Microbacterium[2*,2**]	
		Actinomycetales	*unclassified Actinomycetes* [1**,2**]	
Pseudomonadota	α-Proteobacteria	Sphingomonadales	*Sphingomonas*[1**,2*]	10.35%
	β-Proteobacteria	Rhodocyclales	*Dechloromonas*	
	γ-Proteobacteria	Pseudomonadales	*Pseudomonas*[2*,2**]	
		Enterobacterales	*Pantoea*[1*,1**,2**]	
			Erwinia[2**]	
			Enterobacter[1*,1**]	
			Citrobacter[2**]	
Other Unclassified	Unclassified in lower taxonomic level	Unclassified	*Unclassified environmental spp.*[2**,2*]	13%

[1*]non-polluted young, [1**]non-polluted ripe,[2*]polluted young, [2**]polluted ripe

The class Bacilli was dominant, with genera such as *Bacillus*, *Paenibacillus*, *Priestia*, and *Staphylococcus.Ente robacter*, *Risungbinella* and uncultured *Exiguobacterium* were limited to the non-polluted site, suggesting stress sensitivity. *Curtobacterium* and *Plantibacter* were only isolated from young seeds, while *Brevibacterium*, *Pseudomonas*, *Priestia*, *Streptococcus*, and *Microbacterium* were specific to ripe seeds from both sites (Table 1).

A core endophytic community can be proposed based on a consistent presence in all seed types and environmental conditions a cultivable core endophytic community at the genus level can be proposed, comprising *Bacillus*, *Paenibacillus*, *Pantoea*, *Okibacterium*, *Staphylococcus*, *Micromonospora*, *Peribacillus*, *Promicromonospora* and *Sphingomonas*. Across all conditions, the core bacterial groups were dominated by members of Pseudomonadota, Bacillota and Actinomycetota (Fig. 1). Pseudomonadota represented by, genera like *Pantoea*, *Sphingomonas*. Actinomycetota were represented primarily by *Okibacterium, Micromonospora*, *Promicromonospora*, whereas Bacillota included several abundant and persistent *Bacillus, Staphylococcus*, *Peribacillus*. While the present work defines a stable core seed microbiome at the genus level, the full ASV-based structure of the core community will be explored in a follow-up study to better resolve strain-specific responses to metal stress.

In vitro PGP tests showed that bacterial isolates from ripe seeds (from the polluted and non-polluted site taken together) could produce Indole-3-Acetic Acid (IAA), organic acids (OA), produced siderophores (SID) and exhibited ACC deaminase (ACCD) activity (Figure S1).

However, significant differences between isolates from ripe seeds originating from polluted and non-polluted sites were observed (Fig. 6a).

Strains isolated from the ripe seeds (R) of *O. lutea* growing on the metal polluted site (HM) demonstrated the highest numbers of positive responses for the tested PGP traits regardless of the seed generation (2021, 2022) (not shown). High numbers of siderophore and ACC-deaminase producing bacteria were found in seeds from the polluted soil (Fig. 6b). Strains of genera like *Pseudomonas* spp., *Microbacterium* spp., *Staphylococcus* and *Promicromonospora* isolated from both polluted and non-polluted sites displayed the highest numbers of positive responses for production of siderophores (SID) and ACC deaminase activity (ACCD). Most abundant bacterial groups demonstrated the highest number of positive reactions for production of IAA. Only *Pseudomonas* spp. and *Staphylococcus* displayed the highest number of positive reactions for production of organic acids (OA) (Fig. 6b). Other bacterial groups displayed high numbers of positive reactions only for certain traits, like

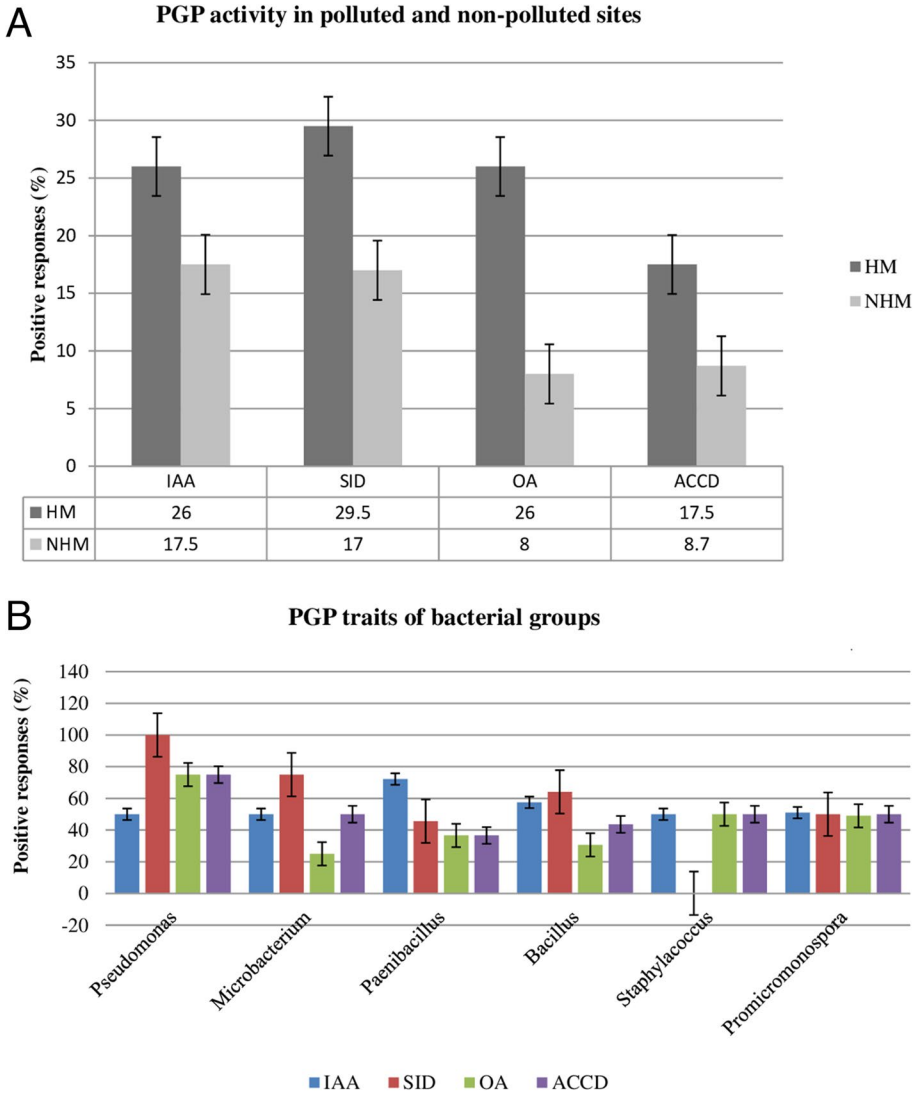

Fig. 6 Plant growth-promoting (PGP) traits for the isolated bacterial groups. **a** The relative abundance of positive responses to four key PGP assays: Indole-3-Acetic Acid (IAA), Siderophores (SID), Organic Acids (OA) and 1-Aminocyclopropane-1-Carboxylate Deaminase (ACCD) across all bacterial isolates. Bacterial isolates from the polluted site (HM) are shown in dark grey, while those from the non-polluted area (NHM) are depicted in light grey. **b** Highest positive responses for the abundant bacterial groups isolated from polluted and non-polluted sites. Data represent the summarized values from the 2021 and 2022 experimental years

production of siderophores and IAA or organic acids or ACC deaminase activity.

Metal tolerance and PGP traits under metal stress

The metal tolerance of endophytic bacterial strains was assessed under in vitro conditions using various concentrations of Zn and Pb. Among the 83 strains isolated from ripe seeds originating from the polluted site (HM), only 63 demonstrated tolerance to the lowest applied concentration of Zn. While, only a few strains belonging to *Bacillus*, *Microbacterium* and *Paenibacillus* demonstrated tolerance to 1 mM Pb. All tested isolates able to growth in Zn-free control media (Table 2)**.** However, significant differences in Zn tolerance were observed among bacterial genera and across Zn concentrations. The four dominant genera such as *Bacillus*, *Paenibacillus*, *Microbacterium* and *Curtobacterium* along with a group of unclassified environmental isolates, displayed the highest overall tolerance. *Bacillus, Curtobacterium* and *Microbacterium* were the most Zn-tolerant, while *Paenibacillus* and the unclassified isolates were more sensitive to higher Zn concentrations. *Bacillus* spp. maintained the highest proportion of tolerant isolates at both 0.6 mM and 1.0 mM Zn. Notably, even at 2.5 mM Zn, several remained viable, indicating strong Zn tolerance. Other genera exhibited consistent but comparatively lower tolerance levels. Several strains like *Bacillus*, *Paenibacillus*

Table 2 Zn and Pb tolerance (n) of endophytic bacterial genera isolated from ripe seeds from both polluted and non-polluted site under in vitro conditions

Zn-Pb treatment	Zn 0mM		Zn 0,6 mM		Zn 1.0 mM		Zn 2.0 mM		Zn 2.5 mM		Pb 1.0 mM	
Bacterial Genera	**HM**	**NHM**	**HM**	**NHM**	**HM**	**NHM**	**HM**	**NHM**	**HM**	**NHM**	**HM**	**NHM**
Bacillus spp.	36	15	30	3	22	2	12	-	8	-	3	-
Paenibacillus	12	8	5	-	4	-	4	-	3	-	4	-
unclassifed environmental samples	8	6	5	-	4	-	3	-	1	-	-	-
Microbacterium	3	2	2	1	2	1	2	-	1	-	1	-
Curtobacterium	4	2	3	-	2	-	1	-	1	-	-	-
Micromonospora	-	2	-	1	-	-	-	-	-	-	-	-
Pseudomonas	-	2	-	1	-	-	-	-	-	-	-	-
Risingbinella massiliensis	-	1	-	1	-	-	-	-	-	-	-	-

*Tolerance was defined based on visible growth under Zn and Pb stress conditions. Values represent the number of colonies (n) of tolerant isolates per genus under each Zn and Pb concentration from the polluted (HM) and non-polluted site (NHM)

and *Microbacterium* able to growth in presence of 1.0 mM Pb (Table 2).

The Zn tolerance of strains originating from the non-polluted site (NHM) was also assessed. Among 63 bacterial strains only a few strains –*Bacillus*, *Microbacterium* sp., *Micromonospora spp. Pseudomonas, Risingbinella massiliensis* demonstrated tolerance to 0.6 mM Zn. Additionally, two strains *Bacillus* sp. and *Microbacterium* sp. were tolerant to 1.0 mM Zn (Table 2).

Discussion

We examined the interactions between the holoparasitic plant *O. lutea* and its environment, focusing on environmental stressors, such as soil metal pollution, and the seed endomicrobiome. Specifically, we investigated the survival strategies of the microbiome and the potential roles in host adaptation in polluted habitats. Current knowledge about the effects of metals on seeds remains limited, particularly concerning the underlying mechanisms of damage. Generally, most plants avoid the accumulation of high concentrations of potentially toxic metals in their seeds to preserve germination potential [45]. However, some plant seeds selectively accumulate different heavy metal ions. For example, peanuts and corn primarily accumulate Pb, while wheat seeds tend to accumulate Zn [46]. Such accumulation may reflect an evolutionary adaptation; whereby toxic metals are sequestered in the seed coat to protect vital metabolic processes. Alternatively, it may indicate a passive accumulation due to the failure of other protective mechanisms in highly polluted environments [46, 47]. Our findings show that *O. lutea* seeds exhibit a remarkable tendency to accumulate Zn and Pb (Fig. 3), which correlates with the high concentration of these metals in the soil. However, in vitro Pb tolerance assays show that only few strains demonstrated tolerance (Table 2). Indeed, the absence of Pb-tolerant endophytic bacterial strains in *O. lutea* seeds suggests that Pb may be predominantly accumulated in the seed coat, thereby limiting the need for Pb tolerance of the bacteria within the internal seed tissues. A similar tendency was observed for Zn (Table 2) as well. Even, strains of *Pseudomonas* spp., *Micromonospora* spp. and *Risungbinella* sp. originating from plants growing on non-polluted soils displayed Zn tolerance only on the lowest concentrations (Table 2). Our findings indicate that enhanced Zn and Pb concentrations in seeds do not necessarily enhance the selection or persistence of metal-tolerant endophytes. On the other hand, increased metal concentrations might lead to a selection pressure, reducing the overall endophytic diversity. Similar trends have been observed in other holoparasitic species. For example, flowers of *O. laxissima* growing in cinnamomic soil habitats in Georgia (Caucasus) exhibited high concentrations of Ni, Zn and Cd [10], suggesting that selective

metal accumulation may be a common strategy among holoparasites to manage with metal stress [1, 9, 10, 48, 49].

In contrast, Ni concentrations in *O. lutea* seeds from the polluted site were notable lower compared to those from the non-polluted site (Fig. 3), indicating a selective exclusion mechanism that varies with growing conditions and soil pollution. This pattern is consistent with findings in other holoparasitic plants. A study on the holoparasitic plants *Phelipanche nowackiana* and *P. nana*, parasitizing *Odontarrhena lesbiaca* in Lesbos (Greece), showed that Ni concentrations declined progressively from tubercles to shoots and flowers, indicating a filtering mechanism that prevents Ni accumulation in reproductive structures [9]. The 'filtering out' of Ni, particularly from vegetative to reproductive tissues supports the hypothesis of a corrective adaptation in hyperaccumulator–pollinator mutualisms, whereby toxic metals are excluded from floral tissues that interact with pollinators [50] as a 'corrective' adaptation tool in the context of the hyperaccumulator–pollinator mutualism, related to the hyperaccumulator-pollinator interaction. This mechanism is further supported by Pavlova and Bani (2019), who reported low Ni concentrations in the anthers and pollen of *P. nowackiana* in Albania [51].

Soil pollution can suppress the immune responses of plants, potentially increasing their vulnerability to parasitic invasion due to synergistic stress effects [10]. On the other hand, the parasite may contribute to lowering the toxic metal concentrations in the host plant, thereby helping to maintain the host's defense mechanisms against metal stress [1, 4, 9, 10]. This interaction not only supports the tolerance of parasitic plants in harsh environments but is also crucial for understanding the survival strategies of holoparasitic species under metal stress.

Influence of environmental pollution and seed maturity on microbial diversity

The hyperaccumulation of metals in plant tissues is influenced by several factors, including the bioavailability of the metals in soil, the activity of metal transporters, the expression of detoxification genes, and the interactions with plant-associated microbiota [52, 53]. Exposure of the plant to metals can also promote the migration of specific endophytes to the aboveground parts of the plant [17].

Our findings indicate that both environmental pollution and seed maturity shape the diversity and structure of seed endophytic communities. While Shannon diversity and microbial richness did not differ significantly across groups, ordination analysis (ADONIS R2 = 0.388) revealed substantial differences in community composition between sites, years, and seed developmental stages (Fig. 4). Notably, bacterial community profiles in 2022 appeared more stable than in 2021, possibly reflecting adaptation or stabilization in response to consistent environmental conditions [19]. This also underscores the possible influence of annual environmental fluctuations on microbial community structure [54].

The seeds of holoparasitic plants may be colonized by microbial communities with functional roles in the early stages of seed conditioning and germination [14, 55, 56]. The increased presence of microbial taxa in mature seeds may be attributed to anatomical changes in fruit structure or to physiological processes occurring during late seed development, which may enhance colonization opportunities [57]. Across all seed samples, the most dominant phyla included Pseudomonadota, Bacillota, and Actinomycetota. Interestingly, Actinomycetota were notably more abundant in young seeds from polluted sites, which was not observed in young seeds from the non-polluted site (Fig. 4). The higher abundance of Actinomycetota in seeds from the polluted site correlates with elevated metal concentrations in the soil [58].

Our results highlight dynamic changes in the diversity of the endophytic bacterial community and relative abundance of bacterial taxa during seed maturation, potentially driven by physiological and anatomical changes in the seed structure that facilitate the colonization by specific bacterial taxa [57]. We assume that this dynamic colonization pattern reflects a complex interaction between the holoparasitic plant and its microbiota, influenced by both internal developmental processes and external environmental pressures, such as metal stress.

In mature seeds of *O. lutea*, colonization by α- Proteobacteria was high regardless of soil pollution. Wiśniewska et al. (2025) [19] demonstrated that in *O. lutea* pistil stigmas the Pseudomonadota (99.25%), mainly Enterobacteriaceae (49.88%) and Pseudomonadaceae (48.28%) were dominant bacterial groups. This supports the hypothesis that certain bacteria may have a selective advantage under metal stress, underscored by the dominance of γ-Proteobacteria, as members of this group are known for their stress response capabilities in polluted sites [59].

Canonical correspondence analysis revealed taxon-specific patterns associated to pollution and seed maturity. For example, *Paenibacillus* (known for its role in nutrient cycling and heavy metal tolerance) was more prevalent in seeds from the polluted site [60, 61] whereas *Stenotrophomonas* was more common in ripe seeds from the non-polluted site (Fig. 5).

Overall, our results indicate that metal stress, environmental and climatic factors (including wind, temperature and rainfall), soil physicochemical properties, the holoparasitic plant species and host genotypes all contribute to shaping the diversity of the seed endophytic community. Further research is necessary to clarify how

these factors, particularly metal stress, environmental and climatic conditions influence the bacterial richness and community shifts during the maturation of seeds of holoparasites.

Culturable candidate core endophytes

Heavy metals in soil can change the structure of plant-associated bacterial communities and their metabolic properties, leading to the selection of the most-adapted strains [40]. Among the culturable seed endophytes, genera such as *Bacillus*, *Paenibacillus*, *Pantoea*, *Okibacterium*, *Staphylococcus* and *Micromonospora* were consistently present across all seed types, suggesting that they can be part of the core seed microbiome. Several were also detected across seed maturation stages and sites, suggesting possible vertical transmission (see below).

Certain genera demonstrated site-specific prevalence, potentially reflecting selection for traits involved in metal tolerance. The genera *Citrobacter*, *Erwinia* and *Kocuria* were predominantly isolated from ripe seeds collected from the polluted site (RP), suggesting their possible adaptation to and/or role in metal stress tolerance of their host plant. The genera *Peribacillus* and *Promicromonospora* were consistently found in both young and ripe seeds from the polluted sites (PY, PR). The genera *Bacillus*, *Paenibacillus*, *Pantoea* and *Staphylococcus* were identified as potential core genera across all samples and might be transferred from generation to generation (Table 1). These bacteria may play key roles in seed physiology and health across different developmental stages and environmental conditions. Specifically, several bacterial strains like *Bacillus* spp., *Paenibacillus* spp., *Curtobacterium* sp., *Microbacterium* spp. and a group of unclassified environmental strains isolated from the ripe seeds demonstrated strong tolerance to high concentrations of Zn and Pb salts (Table 2). Zn is an important trace element, however; elevated Zn levels can be extremely toxic for living organisms [62].

There is a growing body of evidence suggesting that plant-associated microorganisms play a crucial role in protecting plants from excess metal exposure. These microorganisms enhance plant growth and nutrient uptake through mechanisms such as nitrogen fixation, phosphate solubilization, and protection against both abiotic and biotic stresses [52, 63].

In our study, more strains isolated from the ripe seeds of *O. lutea* growing on the metal-polluted site exhibited remarkably higher production of IAA, siderophores, organic acids and ACC deaminase activity compared to those isolated from seeds growing on a non-polluted area, which demonstrated fewer positive responses (Fig. 6). These findings are in line with Truyens et al. (2013) [64] who reported that Cd-tolerant seed-borne endophytes from grasses growing in Cd-polluted areas can support phytoextraction and phytostabilization efforts. This supports earlier findings that heavy metal-tolerant PGP bacteria, including genera such as *Bacillus*, *Pseudomonas*, *Streptomyces*, and *Methylobacterium*, can enhance growth and biomass production in crops by mitigating the harmful effects of metal stress and improving metal tolerance [59, 65]. However, the bacteria inhabited the *O. lutea* immature stigmas from polluted sites demonstrated the less positive PGP traits like auxin production, phosphate solubilization, siderophores production compared to unpolluted ones [19].

In contrast, *Micromonospora* spp. strains isolated from *O. lutea* seeds demonstrated fewer PGP traits compared to those from the seeds of *Cistanche phelypaea* growing in saline marshes with high salt concentrations [33]. This suggests that endophytic *Micromonospora* strains may express PGP traits specific to the stress conditions of their native environment.

Several studies have also reported heavy metal tolerance and PGP abilities of *Sphingomonas*, which is known to maintain its growth and exhibits PGP traits under heavy metal stress, such as the production of phytohormones and suppression of abiotic/biotic stresses [59]. In our study, *Okibacterium* spp. and *Sphingomonas* spp. were only tolerant to lower Zn concentrations and showed the fewest positive responses for the in vitro PGP traits (Fig. 6), indicating that may rely on alternative tolerance mechanisms.

Overall, these findings highlight the complex interplay between metal exposure and the functional potential of bacterial communities within seed microbiomes.

Conclusion

Seed endophytic communities of *O. lutea* were shaped by both environmental pollution and developmental stage of the seeds. Certain bacterial genera were consistently detected across all samples, suggesting the presence of a vertically transmitted core microbiome. The high frequency of plant growth-promoting traits and elevated metal tolerance among isolates from polluted sites emphasizes the resilience and ecological importance of seed endophytes under metal stress conditions.

Overall, *O. lutea* provides a valuable model for exploring the complex host-parasite-microbe-metal interactions and underscores the potential role of holoparasitic plants and their microbiomes in ecological restoration and phytoremediation strategies.

Abbreviations

ACC deaminase- 1	Aminocyclopropane-1-carboxylic acid deaminase
CAP	Canonical Analysis of Principal Coordinates
IAA	Indole-3-acetic acid
ICP-OES	Inductively Coupled Plasma Optical Emission Spectroscopy
PCoA	Principal Coordinate Analysis
PGP	Plant growth-promoting

Supplementary Information

The online version contains supplementary material available at https://doi.org/10.1186/s12870-026-08304-4.

Supplementary Material 1.

Acknowledgements
Sincere thanks to Carine Put for the ICP-OES measurements (UHasselt, Belgium). We thank Dr. Karol Zubek for photo of young and ripe seeds by Nikon SMZ-800 stereoscopic microscope (UJK, Poland).

Authors' contributions
KP analyzed and interpreted the data regarding plant—microbe interactions under metal stress and was the main contributor to the writing of the manuscript. ST performed the methodological and handled the software tools, statistical evaluation, and contributed to the visualization of data. TK performed the statistical analyses and contributed to the figure design and manuscript revision. RP identified plant species and provided the seed materials and contributed to the manuscript editing. KW collected and prepared the seed samples and participated in manuscript review. WK provided laboratory and funding resources and contributing to the manuscript revision. JV conceptualized the study, provided laboratory and funding resources, supervised the research and contributed to manuscript editing.

Funding
This work was financially supported by the Hasselt University grant BOF-BILA, Belgium [BOF21BL12, K.P.; J.V., 2021–2022], the Hasselt University Methusalem project, Belgium [08M03VGRJ, J.V.], the Jan Kochanowski University in Kielce grant, Poland [SUPB.RN.25.231, W.K.]. This study was supported also by the Special Research Fund (BOF – Incoming Mobility), Hasselt University, Belgium [BOF24KV09, K.P.; J.V., 2024]. This work was co-financed by the Minister of Science (Poland) under the "Regional Excellence Initiative" program (project no.: RID/SP/0015/2024/01).

Declarations

Ethics approval and consent to participate
The collection of seed material was conducted in strict accordance with local, institutional, national and international guidelines and regulations. Authorization was granted under permit numbers WPN.I.6400.3.1.2021.AD (Ostra Góra) and WPN.6400.4.2021.MS1.1 (Dąbrowa Górnicza)—issued by the Regional Directors for Environmental Protection in Poland. This study did not involve clinical trials or the use of human or animal materials.

Consent for publication
Not applicable.

Data availability
The datasets during the current study are available in the NCBI Sequence Read Archive (SRA) under accession number PRJNA736981 (https://www.ncbi.nlm.nih.gov/). All herbarium specimens have been deposited in the Herbarium of Jan Kochanowski University in Kielce, Poland (KTC). All seed samples are stored in the Gene Bank of the same institution.

Competing interest
The authors declare no competing interests.

Author details
[1]Department of Microbiology, Nicolaus Copernicus University in Torun, Lwowska 1, 87-100, Toruń, Poland
[2]Centre for Environmental Sciences, Hasselt University, Agoralaan Building D, Diepenbeek 3590, Belgium
[3]Faculty of Chemistry, University of Warsaw, Pasteura1, 02-093, Warsaw, Poland
[4]Centre for Research and Conservation of Biodiversity, Institute of Biology, Jan Kochanowski University, Uniwersytecka 7, 25-406, Kielce, Poland
[5]Department of Microbiology, Institute of Biology, Jan Kochanowski University, Uniwersytecka 7, 25-406, Kielce, Poland
[6]Department of Plant Physiology and Biophysics, Institute of Biological Sciences, Maria Curie-Skłodowska University, Akademicka 19, 20-033, Lublin, Poland

Received: 14 October 2025 / Accepted: 2 February 2026
Published online: 10 February 2026

References

1. Turnau K, Jędrzejczyk R, Domka A, Anielska T, Piwowarczyk R. Expansion of a holoparasitic plant, *Orobanche lutea* (Orobanchaceae), in post-industrial areas – a possible Zn effect. Sci Total Environ. 2018;639:714–24. https://doi.org/10.1016/j.scitotenv.2018.05.189.
2. WickeS, Naumann J. Molecular evolution of plastid genomes in parasitic flowering plants. In: Chaw SM, Jansen RK, editors. Advances in Botanical Research. Academic Press; 2018;85:315–347. https://doi.org/10.1016/bs.abr.2017.11.014.
3. Zagorchev L, Stöggl W, Teofanova D, Li J, Kranner I. Plant parasites under pressure: effects of abiotic stress on the interactions between parasitic plants and their hosts. Int J Mol Sci. 2021;22(14):7418. https://doi.org/10.3390/ijms22147418.
4. Westwood JH. The physiology of the established parasite–host association. In: Joel DM, Gressel J, Musselman LJ, editors. Parasitic Orobanchaceae: Parasitic mechanisms and control strategies. Springer; 2013. p. 87–114. https://doi.org/10.1007/978-3-642-38146-1_6
5. Wakabayashi T, Joseph B, Yasumoto S, et al. Planteose as a storage carbohydrate required for early stage of germination of *Orobanche minor* and its metabolism as a possible target for selective control. J Exp Bot. 2015;66(11):3085–97. https://doi.org/10.1093/jxb/erv116.
6. Hacham Y, Hershenhorn J, Dor E, Amir R. Primary metabolic profiling of Egyptian broomrape (*Phelipanche aegyptiaca*) compared to its host tomato roots. J Plant Physiol. 2016;205:11–9. https://doi.org/10.1016/j.jplph.2016.08.005.
7. Yoshida S, Cui S, Ichihashi Y, Shirasu K. The haustorium, a specialized invasive organ in parasitic plants. Annu Rev Plant Biol. 2016;67:643–67. https://doi.org/10.1146/annurev-arplant-043015-111702.
8. Bani A, Pavlova D, Benizri E, Shallari S, Miho L, Meco M, et al. Relationship between the Ni hyperaccumulator *Alyssum murale* and the parasitic plant *Orobanche nowackiana* from serpentines in Albania. Ecol Res. 2018;33(3):549–59. https://doi.org/10.1007/s11284-018-1593-1.
9. Dimitrakopoulos PG, Aloupi M, Tetradis G, Adamidis GC. Broomrape species parasitizing *Odontarrhena lesbiaca* (Brassicaceae) individuals act as nickel hyperaccumulators. Plants. 2021;10(4):816. https://doi.org/10.3390/plants10040816.
10. Piwowarczyk R, Ochmian I, Lachowicz S, et al. Correlational nutritional relationships and interactions between expansive holoparasite *Orobanche laxissima* and woody hosts on metal-rich soils. Phytochemistry. 2021;190:112844. https://doi.org/10.1016/j.phytochem.2021.112844.
11. Davis CC, Xi Z. Horizontal gene transfer in parasitic plants. Curr Opin Plant Biol. 2015;26:14–9. https://doi.org/10.1016/j.pbi.2015.05.008.
12. Clermont K, Wang Y, Liu S, Yang Z, dePamphilis CW, Yoder JI, et al. Comparative metabolomics of early development of the parasitic plants *Phelipanche aegyptiaca* and *Triphysaria versicolor*. Metabolites. 2019;9(6):114. https://doi.org/10.3390/metabo9060114.
13. Kumar K, Amir R. The effect of a host on the primary metabolic profiling of *Cuscuta campestris'* main organs, haustoria, stem and flower. Plants. 2021;10(10):2098. https://doi.org/10.3390/plants10102098.
14. Miao Y, Zhang X, Zhang G, Feng Z, Pei J, Liu C, et al. From guest to host: parasite *Cistanchedeserticola* shapes and dominates bacterial and fungal community structure and network complexity. Environ Microbiol. 2023;18:11. https://doi.org/10.1186/s40793-023-00471-3.
15. de Andra LA, Santos CHB, Frezarin ET, Sales LR, Rigobelo EC. Plant growth-promoting rhizobacteria for sustainable agricultural production. Microorganisms. 2023;11(4):1088. https://doi.org/10.3390/microorganisms11041088.
16. Mastretta C, Taghavi S, van der Lelie D, Mengoni A, Galardi F, Gonnelli C, et al. Endophytic bacteria from seeds of *Nicotiana tabacum* can reduce cadmium phytotoxicity. Int J Phytoremediation. 2009;11(3):251–67. https://doi.org/10.1080/15226510802432678.
17. Sánchez-López AS, Thijs S, Beckers B, González-Chávez MC, Weyens N, Carrillo-González R, et al. Community structure and diversity of endophytic bacteria in seeds of three consecutive generations of *Crotalaria pumila* growing on metal mine residues. Plant Soil. 2018;422:51–66. https://doi.org/10.1007/s11104-017-3176-2.

18. Piwowarczyk R, Krajewski Ł. *Orobanche lutea* Baumg. (Orobanchaceae) in Poland: revised distribution, taxonomy, phytocoenological and host relations. Biodivers Res Conserv. 2014;34(1):17–39. https://doi.org/10.2478/biorc-2014-0008.
19. Wiśniewska K, Przemieniecki SW, Krawczyk K, Hoffmann A, Piwowarczyk R. Impact of pollution on microbiological dynamics in the pistil stigmas of *Orobanche lutea* flowers (Orobanchaceae). Sci Rep. 2025;15:3382. https://doi.org/10.1038/s41598-024-84717-1.
20. Dobrzańska J. Flora and ecological studies on calamine flora in the district of Bolesław and Olkusz. Acta Soc Bot Pol. 1995;24:357–417.
21. Dziubanek G, Spychała A, Marchwińska-Wyrwał E, Rusin M, Hajok I, Ćwieląg-Drabek M, et al. Long-term exposure to urban air pollution and the relationship with life expectancy in cohort of 3.5 million people in Silesia. Sci Total Environ. 2017;580:1–8. https://doi.org/10.1016/j.scitotenv.2016.11.217.
22. Grodzińska K, Korzeniak U, Szarek-Łukaszewska G, Godzik B. Colonization of zinc mine spoils in southern Poland – preliminary studies on vegetation, seed rain and seed bank. Fragm Flor Geobot. 2000;45:123–45.
23. Mielecka-Kubień Z, Wójcik A. Air pollution and health condition of inhabitants of big cities in Śląskie Voivodship Wiadomości Statystyczne. Polish Stat. 2020;65:39–51. https://doi.org/10.5604/01.3001.0014.2344. (**(In Polish)**).
24. Kiczor, B. Soils. In: Tkaczuk, U. (Ed.), State of the environment in the Świętokrzyskie Voivodeship. Report 2017. Wojewódzki Inspektorat Ochrony Środowiska, Kielce, 135–146 (2017). (In Polish). https://powietrze.gios.gov.pl/pjp/rwms/publications/card/ 549.
25. The International Plant Names Index (IPNI).2022. https://www.ipni.org / Accessed 21 Oct 2025.
26. Thiers B. [continuously updated]. Index Herbariorum: A global directory of public herbaria and associated staff. New York Botanical Garden's Virtual Herbarium. http://sweetgum.nybg.org/science/ih/ Accessed 21 Oct 2025.
27. Markowski R, Buliński M, Góra M, Remisiewicz M. Ginące i zagrożone rośliny naczyniowe Pomorza Gdańskiego = Endangered and threatened vascular plants of Gdańskie Pomerania. Acta Botanica Cassubica; 1, pp. 1–75.Gdańsk: Katedra Taksonomii Roślin i Ochrony Przyrody Unywersytetu Gdańskiego. 2004
28. ZázvorkaJ. Orobanchaceae – zárazovité. In: Slavík B, editor. Květena České Republiky. Praha: Academia; 2000 6;477–513. Pladias-Database of the Czech Flora and Vegetation. https://www.pladias.cz/en/taxon/flora/Orobanche%20lutea. Accessed 8 Feb 2026.
29. Pusch J, Günther KF. Orobanchaceae (Sommerwurzgewächse). In: Hegi G, editor. Illustrierte Flora von Mitteleuropa. Jena: Weissdorn-Verlag; 2009. p. 1–99.
30. Thijs S, Witters N, Janssen J, Ruttens A, Weyens N, Herzig R, et al. Tobacco, sunflower and high biomass SRC clones show potential for trace metal phytoextraction on a moderately contaminated field site in Belgium. Front Plant Sci. 2018;9:1879. https://doi.org/10.3389/fpls.2018.01879.
31. Petrosyan K, Thijs S, Piwowarczyk R, Ruraż K, Vangronsveld J, Kaca W. Characterization and diversity of seed endophytic bacteria of the endemic holoparasitic plant Cistanche armena (Orobanchaceae) from a semi-desert area in Armenia. Seed Sci Res. 2022;1–10 https://doi.org/10.1017/S0960258522000204.
32. Eevers N, Gielen M, Sánchez-López A, Jaspers S, White JC, Vangronsveld J, et al. Optimization of isolation and cultivation of bacterial endophytes through addition of plant extract to nutrient media. Plant Biotechnol J. 2015;8(4):707–15. https://doi.org/10.1111/1751-7915.12291.
33. Petrosyan K, Thijs S, Piwowarczyk R, Ruraż K, Kaca W, Vangronsveld J. Diversity and potential plant growth promoting capacity of seed endophytic bacteria of the holoparasite *Cistanche phelypaea* (Orobanchaceae). Sci Rep. 2023;13:11835. https://doi.org/10.1038/s41598-023-38899-9.
34. Callahan BJ, McMurdie PJ, Rosen MJ, Han AW, Johnson AJ, Holmes SP. DADA2: high-resolution sample inference from Illumina amplicon data. Nat Methods. 2016;13(7):581–3. https://doi.org/10.1038/nmeth.3869.
35. Quast C, Pruesse E, Yilmaz P, Gerken J, Schweer T, Yarza P, et al. The SILVA ribosomal RNA gene database project: improved data processing and web-based tools. Nucleic Acids Res. 2013;41(D1):D590–6. https://doi.org/10.1093/nar/gks1219.
36. Yilmaz P, Parfrey LW, Yarza P, Gerken J, Pruesse E, Quast C, et al. The SILVA and "all-species living tree project (LTP)" taxonomic frameworks. Nucleic Acids Res. 2014;42(Database issue):D643–8. https://doi.org/10.1093/nar/gkt1209.
37. McMurdie PJ, Holmes S. Phyloseq: an R package for reproducible interactive analysis and graphics of microbiome census data. PLoS ONE. 2013;8:e61217. https://doi.org/10.1371/journal.pone.0061217.
38. Davis NM, Proctor DM, Holmes SP, Relman DA, Callahan BJ. Simple statistical identification and removal of contaminant sequences in marker-gene and metagenomics data. Microbiome. 2018;6(1):226. https://doi.org/10.1186/s40168-018-0605-2.
39. Weisburg WG, Barns SM, Pelletier DA, Lane DJ. 16S ribosomal DNA amplification for phylogenetic study. J Bacteriol. 1991;173(2):697–703.
40. Oleńska E, Imperato V, Małek W, Włostowski T, Wójcik M, Swiecicka I, et al. *Trifolium repens*-associated bacteria as a potential tool to facilitate phytostabilization of zinc and lead polluted waste heaps. Plants. 2020;9:1002. https://doi.org/10.3390/plants9081002.
41. Patten CL, Glick BR. Role of *Pseudomonas putida* indoleacetic acid in development of the host plant root system. Appl Environ Microbiol. 2002;68:3795–801. https://doi.org/10.1128/AEM.68.8.3795-3801.2002.
42. Cunningham JE, Kuiack C. Production of citric and oxalic acids and solubilization of calcium phosphate by *Penicillium bilaii*. Appl Environ Microbiol. 1992;58(5):1451–8. https://doi.org/10.1128/aem.58.5.1451-1458.1992.
43. Belimov AA, Hontzeas N, Safronova VI, Demchinskaya SV, Piluzza G, Bullitta S, et al. Cadmium-tolerant plant growth-promoting bacteria associated with the roots of Indian mustard (*Brassica juncea* L. Czern.). Soil Biol Biochem. 2005;37(2):241–50. https://doi.org/10.1016/j.soilbio.2004.07.033.
44. Schwyn B, Neilands JB. Universal chemical assay for the detection and determination of siderophores. Anal Biochem. 1987;160:47–56. https://doi.org/10.1016/0003-2697(87)90612-9.
45. Kranner I, Colville L. Metals and seeds: biochemical and molecular implications and their significance for seed germination. Environ Exp Bot. 2011;72(1):93–105. https://doi.org/10.1016/j.envexpbot.2010.05.005.
46. Stefanov K. Accumulation of lead, zinc and cadmium in plant seeds growing in metalliferous habitats in Bulgaria. Food Chem. 1995;54(3):311–3. https://doi.org/10.1016/0308-8146(95)00052-K.
47. Ilić Z, Mirecki N, Trajković R, Kapoulas N, Milenković L, Sunić L. Effect of Pb on germination of different seed and its translocation in bean seed tissues during sprouting. Fresenius Environ Bull. 2015;24(2a):670–5.
48. Debouba M, Balti R, Hwiwi S, Zouari S. Antioxidant capacity and total phenols richness of *Cistanche violacea* hosting *Zygophyllum album*. Int J Phytomed. 2012;4:399–402.
49. Lachowicz-Wiśniewska S, Piwowarczyk R, Ochmian I, Kapusta I, Bernatek M, Piątek J. Correlated trophic and bioactive activities in the parasite–host relationship – *Phelipanche purpurea* vs. *Achillea arabica* case study. Ind Crops Prod. 2023;204(B):117379. https://doi.org/10.1016/j.indcrop.2023.117379.
50. Stefanatou A, Dimitrakopoulos PG, Aloupi M, Adamidis GC, Nakas G, Petanidou T. From bioaccumulation to biodecumulation: nickel movement from *Odontarrhena lesbiaca* (Brassicaceae) individuals into consumers. Sci Total Environ. 2020;747:141197. https://doi.org/10.1016/j.scitotenv.2020.141197.
51. Pavlova D, Bani A. Pollen biology of the serpentine-endemic *Orobanche nowackiana* (Orobanchaceae) from Albania. Aust J Bot. 2019;67(5):381–9. https://doi.org/10.1071/BT18165.
52. Cuypers A, Remans T, Weyens N, Colpaert J, Vassilev A, Vangronsveld J. Soil–plant relationships of heavy metals and metalloids. In: Alloway BJ, editor. Heavy Metals in Soils. Dordrecht: Springer; 2013. p. 161–93. https://doi.org/10.1007/978-94-007-4470-7_6
53. Thijs S, Langill T, Vangronsveld J. The bacterial and fungal microbiota of hyperaccumulator plants: small organisms, large influence. In: Cuypers A, Vangronsveld J, editors. Advances in Botanical Research. Vol. 83. Cambridge: Academic Press; 2017. p. 43–86 https://doi.org/10.1016/bs.abr.2016.12.003
54. Shade A, Peter H, Allison SD, Baho DL, Berga M, Buergmann H, et al. Fundamentals of microbial community resistance and resilience. Front Microbiol. 2012;3:417. https://doi.org/10.3389/fmicb.2012.00417.
55. Mano H, Tanaka F, Watanabe A, Kaga H, Okunishi S, Morisaki H. Culturable surface and endophytic bacterial flora of the maturing seeds of rice plants (*Oryza sativa*) cultivated in a paddy field. Microbes Environ. 2006;21:86–100. https://doi.org/10.1264/jsme2.21.86.
56. Shade A, Jacques MA, Barret M. Ecological patterns of seed microbiome diversity, transmission, and assembly. Curr Opin Microbiol. 2017;37:15–22. https://doi.org/10.1016/j.mib.2017.03.010.
57. Chesneau G, Torres-Cortes G, Briand M, Darrasse A, Preveaux A, Marais C, et al. Temporal dynamics of bacterial communities during seed development and maturation. FEMS Microbiol Ecol. 2020;96(12):fiaa190. https://doi.org/10.1093/femsec/fiaa190.
58. Shahi A, Aydin S, Ince B, Ince O. Evaluation of microbial population and functional genes during the bioremediation of petroleum-contaminated soil as

an effective monitoring approach. Ecotoxicol Environ Saf. 2016;125:153–60. https://doi.org/10.1016/j.ecoenv.2015.11.029.
59. Jain D, Kour R, Bhojiya AA, Meena RH, Singh A, Mohanty SR, et al. Zinc tolerant plant growth promoting bacteria alleviates phytotoxic effects of zinc on maize through zinc immobilization. Sci Rep. 2020;10:13865. https://doi.org/10.1038/s41598-020-70868-8.
60. White JF, Kingsley KL, Butterworth S, Brindisi L, Gatei JW, Elmore MT, et al. Seed-vectored microbes: their roles in improving seedling fitness and competitor plant suppression. In: Verma S, White JF, editors. Seed Endophytes: Biology and Biotechnology. Cham: Springer; 2019. p. 3–20.
61. Truyens S, Weyens N, Cuypers A, Vangronsveld J. Bacterial seed endophytes: genera, vertical transmission and interaction with plants. Environ Microbiol Rep. 2015;7(1):40–50. https://doi.org/10.1111/1758-2229.12181.
62. Mossa AW, Young SD, Crout NMJ. Zinc uptake and phytotoxicity: comparing intensity- and capacity-based drivers. Sci Total Environ. 2020;699:134314. https://doi.org/10.1016/j.scitotenv.2019.134314.
63. Langill T, Jorissen LP, Oleńska E, Wójcik M, Vangronsveld J, Thijs S. Community profiling of seed endophytes from the Pb-Zn hyperaccumulator *Noccaea caerulescens* and their plant growth promotion potential. Plants. 2023;12(3):643. https://doi.org/10.3390/plants12030643.
64. Truyens S, Weyens N, Cuypers A, Vangronsveld J. Changes in the population of seed bacteria of transgenerationally Cd-exposed *Arabidopsis thaliana*. Plant Biol. 2013;15(6):971–81. https://doi.org/10.1111/j.1438-8677.2012.00711.x.
65. Sánchez-López AS, Pintelon I, Stevens V, Imperato V, Timmermans JP, González-Chávez C, et al. Seed endophyte microbiome of *Crotalaria pumila* unpeeled: identification of plant-beneficial Methylobacteria. Int J Mol Sci. 2018;19(1):291. https://doi.org/10.3390/ijms19010291.

Publisher's Note